

Influence of different concentrations of nicotinic acid on the electrochemical fabrication of copper film from an ionic liquid based on the complexation of choline chloride-ethylene glycol

Hasan F. Alesary^{*a, g}, Hani K. Ismail^{b}, Atheer Hameid Odda^c, Mark J. Watkins^d,
Alhussein Arkan Majhool,^e Andrew D. Ballantyne^f, Karl S. Ryder^g**

^a Department of Chemistry, College of Science, University of Kerbala, Kerbala, Iraq.

^b Department of Chemistry, Faculty of Science and Health, Koya University, Koya KOY45, Kurdistan Region - F.R., Iraq.

^c Department of Biochemistry, Faculty of Medicine, University of Kerbala, Kerbala, Iraq.

^d Department of Physics and Astronomy, University Road, University of Leicester, Leicester LE1 7RH, UK.

^e Department of Pharmacy, Al-Zahrawi University College, Karbala, Iraq

^f Institute for Creative Leather Technologies, University of Northampton, Northampton NN1 5PH, UK.

^g Materials Centre, Department of Chemistry, University of Leicester, Leicester, LE1 7RH, UK.

Corresponding authors email: hasan.f@uokerbala.edu.iq, hani.khalil@koyauniversity.org

Abstract

The use of additives to modulate metal electrodeposition from deep eutectic solvents has, to date, apparently been of little interest given the dearth of such studies in the literature. Here, we have actively investigated the effects of nicotinic acid (NA) on the electrodeposition of copper in a choline chloride (ChCl)-ethylene glycol (EG)-based deep eutectic solvent (DES), (1ChCl:2EG), considered a “green solvent” due to its physiochemical properties. Bright copper deposits were formed when NA was added to the Cu electrolyte, while a dull Cu deposit was produced in its absence. New Cu species were found to have formed in the 1ChCl:2EG-based liquid when NA was added to the electrolyte. A number of analytical techniques, in this instance cyclic voltammetry, chronoamperometry, and chronocoulometry, have been employed to determine the various electrochemical properties, nucleation mechanisms, and kinetics of the Cu species reported herein. The diffusion coefficient for the Ethaline-Cu system was found to be affected by the concentration of NA. An electrochemical quartz crystal microbalance (EQCM) was used to

monitor the current efficiency of the copper deposition in both systems. The morphologies, thicknesses, roughnesses, and crystal structures of the copper electrodeposited from the NA-modified electrolyte were characterised via scanning electron microscopy (SEM), atomic force microscopy (AFM), and X-ray diffraction (XRD), which between them demonstrate that the NA introduced into this system acts as a highly effective brightener, producing highly uniform and smooth copper deposits.

Keywords

Electrodeposition, copper, deep eutectic solvent, nicotinic acid

1. Introduction

The electrodeposition of copper plays a significant role in electronics, principally in the production of printed circuit boards, due to its excellent electrical conduction [1-3]. Additionally, the electrodeposition of copper has been used to replace aluminium as a metal for circuit interconnections [4, 5] and Cu deposits are utilised in the multilayer sandwiches of giant magnetoresistance GMR hard disk read heads [6]. Usually, the electrodeposition of Cu is performed in aqueous electrolytes such as cyanide copper, acid copper, pyrophosphate copper, and neutral copper solutions, generally requiring the use of hazardous chemicals or costly treatment requirements [7, 8]. Electrodeposition of Cu from copper sulphate solution in the presence of polyethylene glycol (PEG) or propylene glycol (PPG) has been studied to some extent [9]. PEG and PPG act as levelling agents; these large molecules are thought to ‘block’ areas of the electrode surface, resulting in a levelling effect. Thus, metal deposition cannot occur on sites otherwise already blocked by organic molecules, where the levelling species are generally present around the raised sites on the electrode surface such that the metal will tend to deposit only in any recesses in its surface, effectively levelling it [10]. Other examples of additives in aqueous media are chemical species such as thiourea and ethylenediaminetetraacetic acid (EDTA) when electroplating copper from aqueous electrolyte [11]; each of these examples acts as a brightener, with EDTA coordinating to the Cu ions and, as a consequence, modifying their electrochemical behaviour in solution. The resultant brightness has been found to depend on the orientation of the surface crystallite deposits in a single given plane. Certain organic species can be linked with the

metal ions and complex formation, refining the metal crystals. Such species typically contain a sulphur atom bound to a carbon, or a carbon-carbon triple bond, $-C\equiv C-$ [12].

Alternative media for electrochemical processing, such as deep eutectic solvents (DESs), have been an area of intense research during the past decade due to the unusual chemistries of metal ions. DESs are liquids composed of either Brønsted or Lewis acids and bases that have a dramatic suppression of melting point when combined together. Typically, these are mixtures of the organic halide salts, such as choline chloride, combined with small hydrogen bonding molecules such as ethylene glycol, glycerol and urea although many others exist [13].

Deep eutectic solvents (DESs) have been selected as alternative electrolytes in metal plating solutions to IL systems [14, 15]. DESs have many interesting physiochemical features, for example, many are essentially of little hazard or are indeed non-hazardous and their components can be sustainably sourced, are safe to use, inexpensive to synthesise, are able to dissolve various metal oxides and salts, are non-flammable, easily biodegradable, and are relatively insensitive to water [16, 17]. Due to these properties, DESs are of intense interest in various fields such as electroplating [18-20], electropolishing [21], metal oxide processing [22], desulfurisation [23] and polymer synthesis [24, 25]. A number of investigations have studied the electrochemical behaviour of Cu deposition from DESs [4, 5, 26, 27]. Abbott et al studied Cu deposition from Ethaline 200, finding that the copper reduction occurs by two separate one electron stages, as opposed to one, two electron process in aqueous media [26]. Roy *et al* [27] studied the influence of water content on the electrochemical deposition of Cu from Ethaline 200. While aqua complexes dominate Cu ion speciation in water [28], DESs are water free (if pure) and low coordination number anionic species dominate. Frisch et al showed that Cu^{2+} forms the complex $[CuCl_4]^{2-}$ in the DES Ethaline 200 [29].

The additives used in metal electroplating from aqueous electrolytes are typically intended to enhance particular properties of these coatings, such as brightness, thickness, corrosion resistance and hardness [30, 31]. The use of additives can strongly affect the surface morphology and composition of the deposit, thus influencing its mechanical and electrical properties. Generally, additives fall into two classifications: they can be ligands such as EDTA, which coordinate metals ions resulting in an alternative structure and differing electrochemical behaviour, or small

molecules such as boric acid and nicotinic acid, which adsorb on the electrode surface and inhibit metal deposition in that location, thus affecting the mechanism by which an electrodeposited film nucleates and grows [15, 32, 33]. There have been some studies investigating the effects of additives on the electrodeposition of other metal films, such as nickel and zinc where the additives nicotinic acid, methyl nicotinoate, 5,5-dimethylhydantoin, hydantoin, and boric acid were demonstrated to modify electrochemical deposition behaviour [18, 31, 34]. However, additive effects on Cu electrodeposition from DESs have yet to be investigated in any real detail.

This study investigates the Cu electrodeposition process, with an emphasis on the role of additives on electrocrystallisation. Other recent studies on copper electrodeposition from DES electrolytes have focused on the effect of small molecules such as water [27], and Akolkar *et al* studied the use of polyethylenimine [35]. However to our knowledge, this is the first study on the influence of additives on copper electroplating from choline chloride based ionic liquid, specifically in this case the influence of nicotinic acid (NA) on the electroplating of Cu on a mild steel substrate from a DES based on choline chloride (*a quaternary ammonium salt*) mixed in a ratio of 1:2 with ethylene glycol (*a hydrogen bond donor*) [36, 37]. Initially the conductivity and viscosity of the additive in pure electrolyte (Ethaline) and with added NA have been measured (supplementary data). Following this, the Cu ion speciation with/without the presence of NA will be examined via a UV-vis spectrophotometer. Finally, we studied the effects of different concentrations of NA on the morphology of subsequent Cu coatings, as obtained through cyclic voltammetry, chronoamperometry, chronocoulometry, and electrochemical quartz crystal microbalance (EQCM). Copper electrodeposition from a choline chloride-ethylene glycol ionic liquid has been investigated as a function of the concentration of NA in the plating bath. SEM/EDX and atomic force microscopy (AFM) were used to verify whether NA has an effect as a brightener or levelling agent on the Cu deposit from the DES. Finally, XRD was used to verify that pure Cu deposits were produced.

2. Experimental

Choline chloride [$\text{HOC}_2\text{H}_4\text{N}(\text{CH}_3)_3\text{Cl}$] (ChCl) (Aldrich, 99%) and Ethylene glycol (EG) (Aldrich, > 99%), were used as received. The two components (that form a 1:2 molar ratio of ChCl:ethylene glycol) were mixed by stirring at 60°C until a homogeneous, colourless liquid (Ethaline 200) formed. 0.3 M $\text{CuCl}_2 \cdot 2\text{H}_2\text{O}$ was prepared by adding the copper salts, $\text{CuCl}_2 \cdot 2\text{H}_2\text{O}$ (Aldrich, $\geq 98\%$), to the liquid (Ethaline 200). The additive, nicotinic acid (NA) (Sigma, $\geq 99.5\%$), was used as received.

To record UV-vis spectra, a UV-vis spectrophotometer (Shimadzu model UV-1601) was loaded with a standard sample cuvette with a path length of 10 mm. λ_{max} was determined in each instance using the spectrophotometer's built-in peak pick feature as part of the UV-probe software. Cyclic voltammetry was performed using a potentiostat (Autolab/PGSTAT12) controlled via the GPES2 software. A three-electrode system consisting of a platinum working electrode (1 mm), a platinum foil counter electrode, and a silver wire pseudo-reference electrode was used. Ag wire was used as a pseudo-reference electrode directly immersed into the solution of DESs (Ethaline) and ionic liquid. The reason is that Ag/AgCl RE is not suitable for use in DESs as it can give problems when silver ions leach from the reference electrode. Further, there is a high concentration of Cl^- ions in DESs (13% Cl^- ion in Ethaline). Cl^- ions surround the Ag wire which is immersed into the DESs. Therefore, the probable reaction of Ag wire pseudo RE is between Ag and AgCl the same as Ag/AgCl RE in aqueous solution [24, 38]. All cyclic voltammograms were recorded at 70°C at a number of scan rates between $10\text{-}70 \text{ mV s}^{-1}$.

Electrochemical Quartz Crystal Microbalance (EQCM) technique was used to measure current efficiency of the copper deposits, where this was obtained utilizing a Hewlett Packard (HP) 8751A 5 Hz-500 MHz network analyser connected to a computer (software) and an Autolab III potentiostat. In his experiment a conventional three-electrode were performed in a locally constructed teflon cell. The counter and reference electrodes were identical to those used in the CV experiments, while the working electrode was a 10 MHz AT-cut quartz crystal polished coating with Platinum (Pt) one side and gold (Au) on the other (International Crystal Manufacturing Co., Oklahoma City, USA, mounted). The electrochemical and piezoelectric active areas were 0.23 cm^2 and 0.21 cm^2 , respectively. In the assembled cell, the Pt electrode was exposed

to the solution whilst the other (Au) side was exposed to air. The measurement was recorded at -0.4 V for the Cu deposited at 70 °C.

Bulk electrodeposition was performed using cathodic plates (mild steel, 15 mm \times 30 mm \times 1 mm) that had been mechanically polished and subsequently cleaned by rinsing with acetone followed by water, and which were then thoroughly dried. Titanium mesh electrode (50 mm \times 60 mm) was used as the anode, and was prepared in the same manner. All electrodeposition experiments were performed at 70 °C at a constant current of 2 mA cm⁻² for 1 hour. The substrates were then removed from plating bath and washed using water and acetone. Surface morphologies and compositions were characterised via scanning electron microscopy (SEM) and energy dispersive X-ray spectroscopy (EDX) (Phillips XL30 ESEM) using an accelerating voltage 20 keV. To determine the cross-sectional microstructure, samples were mounted in a resin using an appropriate press (Struers Labo Press 3), then refined with silicon carbide paper (240 grit) to give them a flat surface and then successively with 9 μ m and 3 μ m size diamond abrasives, followed by a final treatment with a 0.5 μ m colloidal silicon carbide paste. The surface roughness of the Cu deposits was measured using AFM-Dimension 300 (Veeco). A Phillips model PW 1730 X-ray generator, with a PW 1716 diffractometer and PW 1050/25 detector, was used to examine the crystal structures of the Cu coatings.

3. Results and discussion

3.1. Speciation

Metal ion speciation is dependent on the associated chemical environment. In water, $\text{CuCl}_2 \cdot 6\text{H}_2\text{O}$ forms an octahedral hexa-aqua complex $[\text{Cu} \cdot 6\text{H}_2\text{O}]^{2+}$, whereas in Ethaline 200 a tetrahedral $[\text{CuCl}_4]^{2-}$ complex forms. Here, UV-Vis spectroscopy was used to determine whether there were any changes in speciation for $\text{CuCl}_2 \cdot 2\text{H}_2\text{O}$ in Ethaline 200 with the introduction of NA. **Fig. 1a** shows the UV-Vis spectrum of 0.40 mM of $\text{CuCl}_2 \cdot 2\text{H}_2\text{O}$ in Ethaline 200 containing increasing concentrations of NA (0 , 0.10 , 0.15 , 0.20 mM) recorded at 70 °C. Three peaks can be observed at 240 , 300 and 410 nm, previously identified as occurring due to charge transfer transitions characteristic to the speciation of many metal ions in DESs, where the resulting solvated structure is dominated by the high chloride concentration.

There is a corresponding colour change when visually observing the solutions containing increasing quantities of NA, as shown in **Fig. 1a**. A 0.40 mM concentration of $\text{CuCl}_2 \cdot 2\text{H}_2\text{O}$ in Ethaline 200 formed a yellow solution in the absence of NA, but gradually changed to a less intense yellow/green with increasing concentrations of NA [26]. The yellow colour originates from the absorption of low wavelength visible light, likely the peak observed at 410 nm in the UV-vis spectrum. The yellowish-green could be attributed to the formation of new complexes as a result of the addition of the additive. In **Fig. 1a** that there are absorption peaks in the ultraviolet at ~300 nm, and in the visible at ~410 nm; two absorption maxima are present at 406 and 291 nm for the $\text{CuCl}_2 \cdot 2\text{H}_2\text{O}$ solution without NA that correspond to $[\text{CuCl}_4]^{2-}$ formation, as corroborated by EXAFS [27, 28, 39]. The band at 406 nm gradually decreased in intensity with increasing concentration of NA, indicating that $[\text{CuCl}_4]^{2-}$ is steadily reduced. The absorption feature at 291 nm was observed to shift towards the blue and to reduce in intensity with increasing concentrations of NA due to the reduction in $[\text{CuCl}_4]^{2-}$ with the formation of an additional species that incorporated NA. It is worth noting here that the concentrations of both concentrations of CuCl_2 and NA as well as their relative concentrations are lower than that of the concentrations used for deposition studies below as absorption would be too high. However, this does provide useful information regarding the behaviour of Cu^{2+} ions in the DES Ethaline 200 with and without the presence of NA, demonstrating that there is Cu ion complexation by NA.

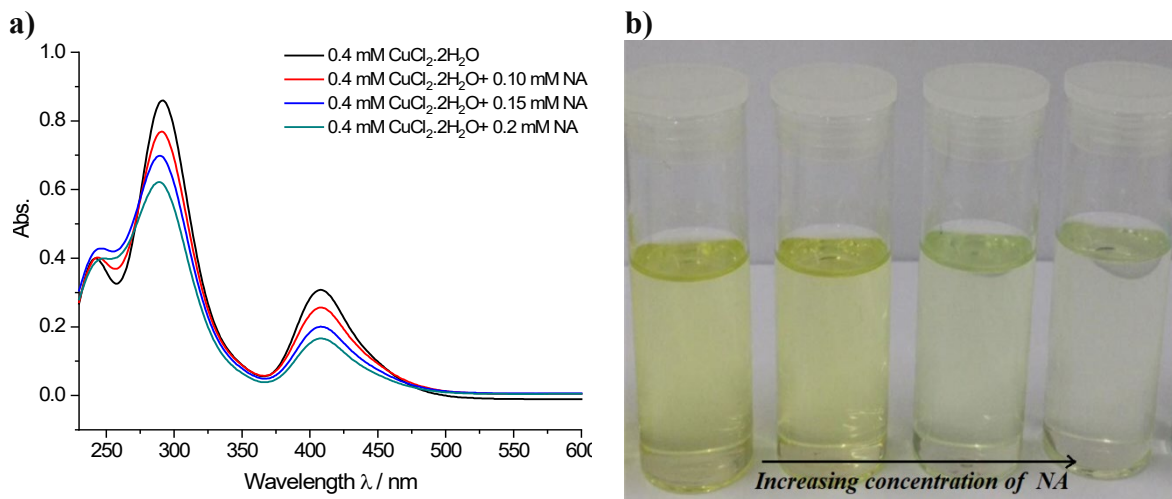


Fig.1. a) UV-Vis spectra and **b)** colour changes of a 0.4 mM electrolyte of $\text{CuCl}_2 \cdot 2\text{H}_2\text{O}$ in Ethaline with various concentrations of NA recorded at 70°C.

No structural determinations of Cu(II) species complexed by NA could in DES could be found in literature. However, aqueous studies observed that mono and bi-dentate species may form, at various levels of carboxylate protonation depending on pH [40]. Solid state studies show that complexation occurs through the pyridine nitrogen atom [41]. Given the Cu is in excess at the concentration of study it is likely that one NA complexes with each Cu(II) ion through the N pyridine atom, though further work is required.

3.2. Cyclic voltammetry study

3.2.1. Effect of NA Additive Concentration on the CV of Cu(II)

Fig. 2 shows cyclic voltammograms (CVs) of 0.3 M CuCl₂·2H₂O in 1:2 ChCl:Ethylene glycol-based DES containing various concentrations of NA at 70°C, recorded at a constant scan rate of 30 mV s⁻¹ on a Pt working electrode in the potential range of 1.0 V to -1.0 V (vs. Ag wire), as presented in **Fig. 2**. The CV graphs show that there are two stages of redox reactions for copper (II) in the choline chloride and ethylene glycol mixture, where the reversible reduction peaks are attributed to the reduced reactions of Cu²⁺ to Cu⁺ at +0.41 V (peak 2, equation 1) followed by Cu⁺ to Cu⁰ at -0.38 V (peak 1, equation 2), the deposition of metallic copper [26, 42]. It is noted that peak potentials given are used for the purpose of describing the CV's obtained in **Fig. 2**. As an Ag wire pseudo reference was used in the absence of a Luggin capillary, as well as the capacity to react with Cu(II) ions, that the true values are likely to be different. The observed CV is similar to that of other papers studying the electrodeposition of Cu in DES media where two distinct peaks are observed [26], as the Cu⁺²⁺ redox couple is significantly more anodic than the Cu^{0/+} one. This has been attributed to the stabilisation of low coordination number, low oxidation state species for metal ions when compared to aqueous media, observed through EXAFS speciation studies [43]. During this work no attempt were made to measure moisture content as electrochemical measurements were undertaken in open apparatus at 70 °C having been stored in a closed bottle at room temperature after their preparation. However, van Deun *et al* demonstrated that Cu(II) speciation in Ethaline 200 remained consistent up c.a. 50 wt% moisture in a 0.1 mol L⁻¹ CuCl₂ solution [28], while Dela Pena *et al* showed that elevated temperatures significantly reduced moisture content [44], suggesting that trends observed here should be consistent across low to moderate moisture contents.

A trend may be observed from the CV graphs that with increasing concentrations of NA, the deposition potential of Cu (Cu^+ to Cu^0) shifts towards negative values (see potential peaks in **Table 1**), and the deposition current becomes markedly lower with increasing NA concentration. At 0.06 M, the highest concentration of NA, there is 6-fold reduction in the peak current. This demonstrates that deposition is inhibited when the additive is present. A nucleation ‘loop’ is obtained in the deposition peak of Cu when the voltammograms recorded from system without NA, as shown in **Fig. 2**, but was not observed when using NA additive in the CuCl_2 electrolyte. This is indicative of the nucleation rate for the Cu deposition being faster than that for Cu deposition from the systems containing NA. This impedes the growth of Cu nuclei, thus reducing the intensities of the Cu reduction and oxidation current peaks, as illustrated in **Fig. 2**.

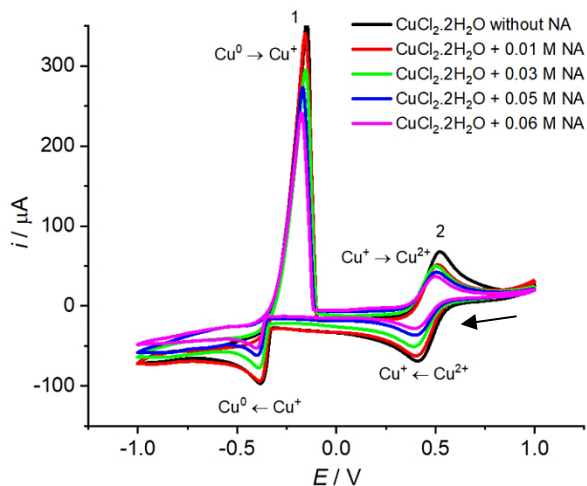


Fig. 2. Cyclic voltammogram of 0.3 M $\text{CuCl}_2 \cdot 2\text{H}_2\text{O}$ in 1:2 ChCl:Ethylene glycol-based ionic liquid containing various concentrations of NA at 70°C

Inhibition of Cu reduction / deposition may occur through many reasons. Firstly, there is a composition change present with increasing concentration of NA, which will have a corresponding influence of the viscosity, resulting in a change in the diffusion coefficient, linked through the Stokes-Einstein equation (eqn. 3) [45], where D is the diffusion coefficient, k_B is the Boltzmann constant, T is the temperature in Kelvin, η is the viscosity and R_0 the solute radius. It can be observed from **Table 1** that the viscosity of these solutions increases with increasing NA.

However, this change is only small, and not enough to cause the large reduction in peak currents observed here for both solution phase and deposition processes. Secondly, there may be a change in speciation due to NA coordination with the Cu ions, leading to an increase in the solute radius and / or modification electrochemical behaviour. UV-Vis measurements, shown in **Fig. 1**, demonstrate that some speciation change does occur in the presence of NA. However, this does not provide sufficient explanation of the change in electrochemical behaviour as the maximum concentration of NA is only 20% of the concentration of Cu²⁺ ion in solution. Lastly, the NA may inhibit electrochemical processes either through the formation of transient species close to the electrode surface that alter electrochemical reaction or may adsorb onto the surface influencing the kinetics of nucleation and growth [46, 47]. It seems likely that it the latter two mechanisms that affect the electrochemical behaviour here; through identifying which of the two mechanisms is dominant is difficult. It is likely that the two electron transfer processes observed here, are limited by the presence of NA coordinating to the substrate surface, indicating that the NA may act as a brightener Cu deposition, media through binding to the substrate surface, in a similar manner to Ni deposition from the same DES and aqueous deposition of copper [46, 48].

$$D = \frac{k_B T}{6\pi\eta r} \dots\dots\dots 3$$

As mentioned, peak 2 in **Fig 2** shows a redox couple for Cu⁺/Cu²⁺. Interestingly, the presence of NA results in a significant reduction in the peak current for both the cathodic and anodic waves of the CVs as well as an increase in the peak separation of the respective waves.

Table 1 details the peak current and viscosity of respective solutions.

Solution (0.3 M [CuCl ₂ .2H ₂ O] in Ethaline 200)	<i>i_p</i> A Cu ²⁺ /Cu ⁺	Viscosity (cP) at 70°C
Cu ²⁺ /Cu ⁺ in water	-	0.4045[49]
Cu ²⁺ /Cu ⁺ in Ethaline	7.528×10 ⁻⁵	13.33
Cu ²⁺ /Cu ⁺ in Ethaline +0.01 M NA	7.160×10 ⁻⁵	13.73
Cu ²⁺ /Cu ⁺ in Ethaline +0.03M NA	5.578×10 ⁻⁵	13.93
Cu ²⁺ /Cu ⁺ in Ethaline +0.05 M NA	4.555×10 ⁻⁵	14.26
Cu ²⁺ /Cu ⁺ in Ethaline +0.06 M NA	1.222×10 ⁻⁵	14.41

To further study the nucleation and growth from these solutions, chronoamperometry was performed. **Fig. 3** shows chronoamperometry responses of Cu deposition from a 0.3 M

$\text{CuCl}_2 \cdot 2\text{H}_2\text{O}$ solution in Ethaline where all experiments were achieved with a Pt disc electrode at 70°C at -0.3 V in the presence of no, 0.01 M , 0.03 M and 0.05 M NA, as referenced to Ag wire. After an initial sharp drop in the current magnitude due to charging of the electrode double layer upon initiation of the experiment, each of the transients show a peak due to nucleation and growth of nuclei on the electrode surface. After the nucleation peak the current decays due to transition from three-dimensional nucleation/growth to one-dimensional diffusion-limited growth. In all cases where NA was present, the nucleation occurred within a shorter timescale than when there was no NA present.

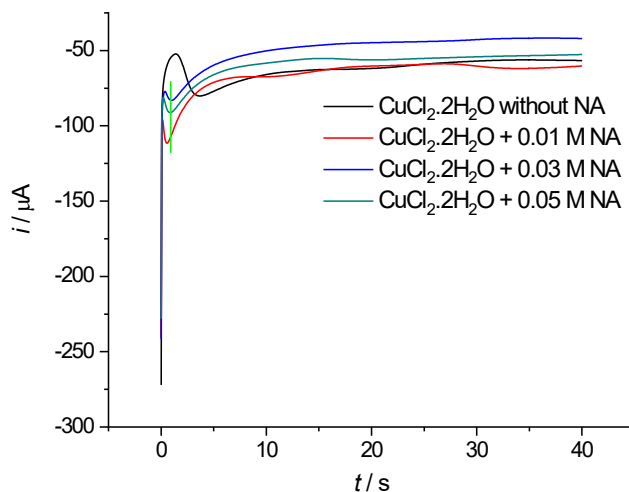


Fig.3. Current-time transients resulting from chronoamperometric experiments for the electroreduction of Cu (II) on a platinum electrode at -0.3 V vs. Ag wire

3.2.2. Effects of Scan Rate on the CV of Cu with/without nicotinic acid

The effects of the addition of NA additive on the Cu deposition on the Pt working electrode were examined at various scan rates in 1ChCl:2EG-based liquid containing 0.3 M $\text{CuCl}_2 \cdot 2\text{H}_2\text{O}$ with/without 0.03 M NA at high temperature (70°C), as demonstrated in **Fig. 4a** and **c**. In this study, the potential window for the CVs in each of the above systems ranged from (a starting potential of) 1.0 V and was run to -1.0 V . This was then run in reverse to the starting point. In general, this experiment shows increasing in current peak intensities in both the anodic and cathodic areas with increasing scan rate for both systems (i.e., before and after the addition of NA to plating bath). Similar findings have been described elsewhere [33]. However, it is interesting to note that the currents of the voltammograms (**Fig.4a** and **c**) in each of the systems are entirely different. The current value for the Cu^+/Cu^0 couple in the presence of NA additive at all scan rates

was somewhat smaller than for the same system without this additive. Here, we have observed the difference values in separation for potential peaks of $\Delta E_p = 269$ mV and $\Delta E_p = 256$ mV for the redox of Cu^0/Cu^+ species in the absence and presence of additive, respectively (calculated from the results presented in **Fig. 4a** and **c**). This data is bigger than the $59/n$ mV anticipated for a reversible system [50], indicating that the ratios of the peak current for anodic–cathodic processes are quite independent of scan rate, and thus that the electron transfer process is not reversible regarding the redox region Cu^0/Cu^+ . To clarify this mechanism, the reversibility of the dissolution and deposition of Cu on the Pt electrode was conveniently evaluated in this experiment. It was found that the plots of current density ($j / \text{A cm}^{-2}$) for $\text{Cu}^+/\text{Cu}^{2+}$ species (anodic direction) and its reversible $\text{Cu}^{2+}/\text{Cu}^+$ (cathodic direction) versus the square root of scan rate (V s^{-1}) are linear in both systems, suggesting that the reactions are controlled by diffusion processes [51], as shown in **Fig. 4b** and **d**. In addition, we will discuss this supposition in more detail in the following section.

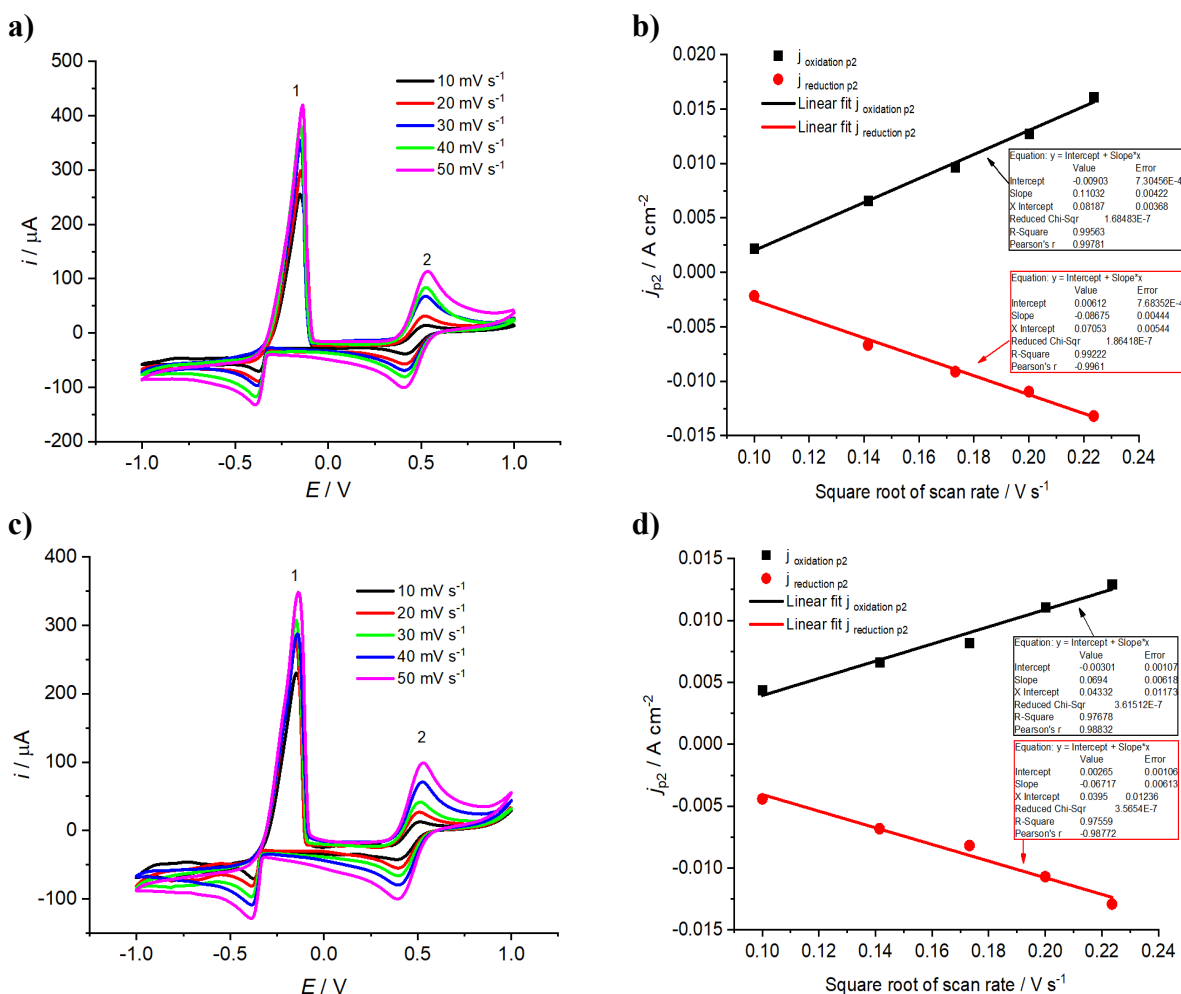


Fig. 4. Effect of scan rate on cyclic voltammograms for a Pt disc (1.0 mm diameter) electrode immersed in 1ChCl:2EG based liquid in the presence of 0.3 M [CuCl₂·2H₂O] (a) without NA (c) with 0.03 M NA. Redox current density for 0.3 M [CuCl₂·2H₂O] (b) without NA and (d) with NA 0.03 M MN additive in Ethaline 200 as a function of the square root of the scan rate.

3.3. Chronocoulometry study

To confirm the diffusion mechanism of Cu electrodeposition in both systems (i.e., with/without different concentrations of additive), the chronocoulometry experiment for 0.3 M [CuCl₂·2H₂O] was studied in both systems in the 1ChCl:2EG-based liquid using a Pt working electrode (dia. 1 mm), as displayed in **Fig. 5**. The potential was held at +1.00 V (for 10 s) then stepped to -1.0 V for 30 min. It can be observed from **Fig. 5** that there are linear responses from the plot of Q versus $t^{1/2}$ for all experiments (i.e., both with and without additive), suggesting that the processes in both systems are diffusion controlled. Similar findings for Cu deposition in Reline and Ethaline have been described elsewhere [26]. Additionally, the charge continually increases with time because the charge obtained is directly proportional to the number of moles (N) of the deposited species according to Faraday's Law ($Q = nFN$) [52]. However, it should be noted that the magnitude of charge reduces with increasing concentration of NA additive in the plating electrolyte. This may be due to higher concentrations of additive species blocking the Cu⁺ ion from the electrode surface, preventing it from being reduced and depositing (Cu⁰) on the polished Pt surface. As a result of these data, the current efficiency for the Cu deposition containing additive will be lower for the additive-free electrolyte, which is most noticeable in the EQCM results.

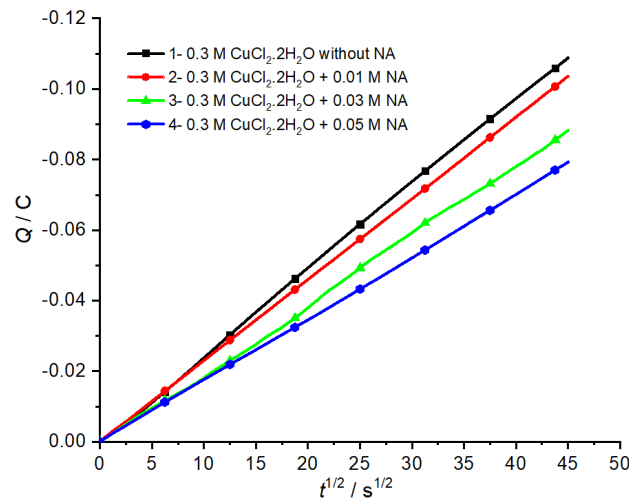


Fig. 5. Chronocoulometry data for 0.3 M CuCl₂·2H₂O with and without various concentrations of NA on a 1.0 mm diameter Pt wire in the 1ChCl:2EG-based liquid for potential steps from 1.00 V for 10 s followed by a step to -1.00 V for ca. 1800 s. (1.0 mm diameter Pt wire)

3.4. Gravimetric Study

In the previous sections, the effect of NA additive on Cu growth and its rate of deposition from Ethaline at 70°C were investigated by cyclic voltammetry and chronocoulometry, demonstrating that the presence of NA inhibits the rate of Cu deposition. It is likely that NA achieves this through two possible mechanisms: complexation with the Cu ions in solution, and absorption onto the Pt substrate surface inhibiting deposition at some sites on the surface. Here we determine the charge-mass balance for Cu deposition with/without the additive and calculate the current efficiency of Cu under these conditions using an electrochemical quartz crystal microbalance (EQCM), for which representative results are presented in **Fig. 6**.

EQCM monitors and determines mass changes due to chemical species deposited on a quartz crystal substrate of an electrode through acoustic impedance. The change in resonant frequency of the quartz crystal electrode is linearly related to the mass deposited on the electrode surface through the Sauerbrey equation [53], equation 2.

$$\Delta f = \frac{2f_0^2}{A\sqrt{\rho_q\mu_q}} \Delta m \dots\dots\dots 2$$

Here, $\Delta f/\text{Hz}$ is the change in frequency due to the deposition of a mass $\Delta m/\text{ng}$. f_0/Hz is the resonant frequency of the quartz crystal, A/cm^2 its active face area, $\rho_q/\text{g cm}^{-3}$ is the density of quartz, and $\mu_q/\text{g cm}^{-1} \text{ s}^{-2}$ the quartz shear modulus for an AT-cut quartz crystal. Here, the Cu compound (0.3 M CuCl₂) with/without different concentrations of NA (0.01-0.05 M) was electrochemically deposited onto the polished electrode of a Pt-coated (10 MHz) AT-cut quartz crystal from 1ChCl:2EG-based electrolytes using a constant potential of -0.38 V at a fixed 70°C bath temperature. The data illustrated in **Fig. 6b** describes the relationship between Cu mass vs. the total charge passing during formation in the Ethaline 200. The theoretical molar mass (M) of Cu

is 63.55, whilst the experimental value, as determined from the plot of mass vs. charge illustrated in **Fig. 6b** and explained by Faraday's law, is given by equation 3.

$$\frac{\Delta m}{\Delta q} = \frac{M}{zF} \dots\dots\dots 3$$

where $\Delta m/g$ is the mass deposited, $\Delta q/C$ is the change in charge, z is the number of electrons lost and gained (here equal to 2), and F is the Faraday constant ($96,485 \text{ C mol}^{-1}$). The 'real-world' M can be determined by simple rearrangement of equation 4:

$$M = \frac{zF\Delta m}{\Delta q} \dots\dots\dots 4$$

Consequently, the current efficiency for Cu deposition with/without additive can be simply calculated from the experimental M (**equation 4**) divided by the theoretical value of Cu (63.55). The current efficiency for pure Cu coating was found as 94.52%, which is close to the data reported in the literature [26, 46]. On the other hand, the value of the current efficiency for the Cu coating decreased to 86.88% when the deposition was carried out in the presence of 0.01 M NA additive and is further significantly decreased with increasing concentration of additive in the plating bath, as shown in **Table 2**.

From the results of **Fig. 6**, utilising NA yielded a decrease in the rate of deposition for Cu on the electrode surface in comparison to pure Cu deposition. One can interpret this as due to the adsorption of the additive onto the active sites of the surface increasing with increasing concentration of NA, which will impede further copper deposition, leading in turn to a decrease in current efficiency. In the case of the data for the mass change vs. timescale (1500 s) for Cu deposition with the NA additive, it can be seen from **Fig. 6a** that the mass is increased significantly compared to that found for pure Cu metal deposition; this can simply be interpreted as the codeposition of the NA additive with the copper. These values are strongly dependent on the frequency of the quartz crystal and are affected by the concentration of species in the plating bath; therefore, there is a large decrease in the quartz crystal frequency such that the mass can be said to have increased considerably more than for the additive-free Cu deposition. It can be concluded that the EQCM data provide further support for the role of adsorption/codeposition of the NA onto the active points of the electrode, thus inhibiting Cu deposition. This, in turn, results in a decline

in the current efficiency of the copper coating on the electrode in the plating solution. A similar approach has recently been reported for the electrodeposition of alloys and other metals in DES systems [46, 54]. The faradaic processes that arise due to the reduced current efficiency require further study. However, when studying Zd electrodeposition from the same liquid Haerens *et al* identified 2-methyl-1,3-dioxolane, acetaldehyde and a small amount of chloroform as decomposition products at the cathode [55]. In addition, it may be that not all Cu^{2+} ions are reduced to $\text{Cu}(0)_{(s)}$ given the action of the additive to block deposition sites at the anode surface and $\text{Cu}^{(+)}$ ions diffuse away from the electrode surface to bulk solution.

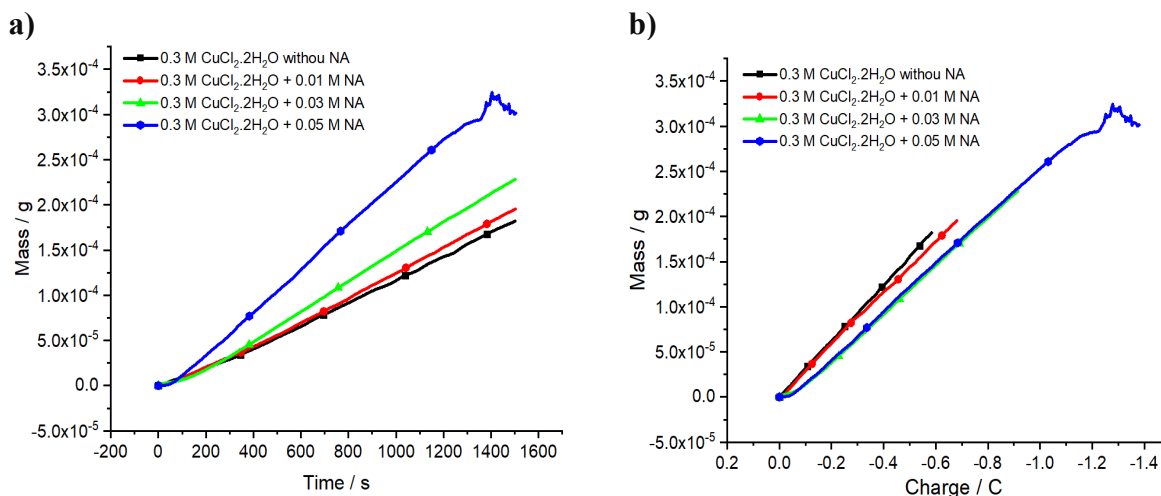


Fig. 6. Gravimetric data for the electrodeposition of Cu on a Pt-polished quartz crystal (10 MHz) electrode for **a)** mass vs. time and **b)** mass vs. charge. The investigations were achieved in 0.3 M CuCl_2 in Ethaline 200 at 70°C in both the absence and presence of different concentrations of additive. The applied potential was -0.38 V vs. an Ag wire reference electrode for 1500 s.

Table 2 Efficiencies of Cu deposition onto a Pt-coated quartz crystal (10 MHz) in Ethaline 200 at 70°C containing 0.3 M CuCl_2 with/without various concentrations of NA additive at a voltage of -0.38 V , as determined from EQCM data.

Samples	$\Delta m(\text{g})$	$\Delta q(\text{C})$	$M. (\text{g C}^{-1})$ practically	Reduction current efficiency %
(1ChCl:2EG): 0.3 M CuCl_2	1.821×10^{-4}	0.585	60.07	94.52
(1ChCl:2EG): 0.3 M CuCl_2 :0.01 M NA	1.954×10^{-4}	0.683	55.21	86.88
(1ChCl:2EG): 0.3 M CuCl_2 :0.03 M NA	2.28×10^{-4}	0.916	48.03	75.58

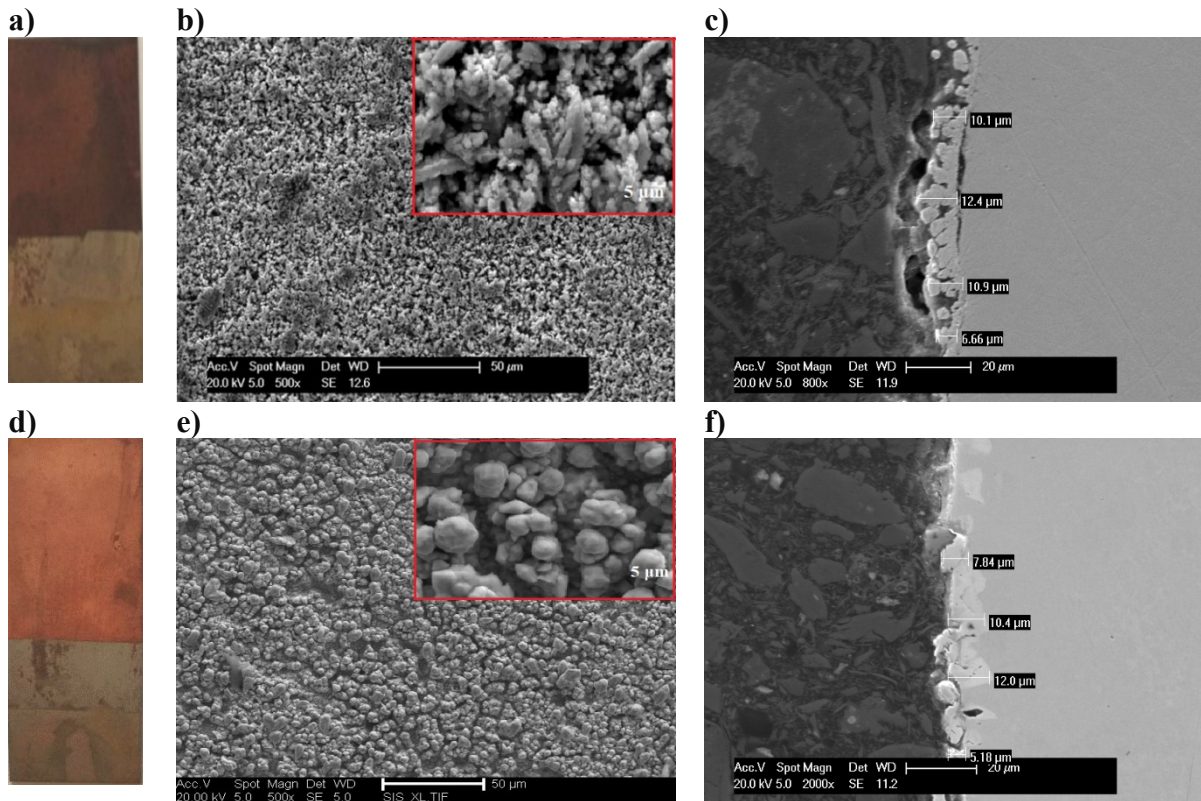
3.5. Surface Characterisation

Fig. 7 shows the optical photographs (left), SEM morphologies (middle), and cross-sectional images (right) for Cu electrodeposition without/with various concentrations of NA in a 0.3 M CuCl₂.2H₂O/Ethaline 200 electrolyte at a fixed bath temperature of 70°C. In all experiments, the current density was held at 2 mA cm⁻² and electroplating was carried out for 1 hour on mild steel substrates. Indeed, good adherence and highly uniform thicknesses were achieved for all Cu coatings with/without additive. In the electrodeposited additive-free Cu film, the morphology of the film was found to be a rough layer with larger grains, as shown in the inset of **Fig. 7b**.

However, we note that the surface morphologies for the Cu deposits change with the addition of the NA additive to the Cu plating bath (**Figs 7e, h, and k**). Obviously, the sizes of particles were notably reduced, and the particle grains gradually become smaller with increasing amounts of NA additive in the plating solutions; the surface morphology becomes increasingly smooth and homogeneous with concentration in comparison to the Cu deposition without NA. This is a result of a reduced crystal size due to the addition of [different concentrations of] NA additive. This suggests that NA may work as the grain finer for film deposition, which would lead to a reduction in growth rate of the Cu deposit. These results are in agreement with those obtained by Gu at el [56]. It is obvious that the Cl⁻ ions from Ethaline 200 may have a small influence, however, the concentration of NA additive was key to the impact on the morphology of the copper layer. This implies that the activity of the Cu surface has been improved toward nanoporous and granular surfaces.

It is clear that the optical photographs (left) show that the brightness of the Cu surfaces increased with increasing concentration of additive in comparison with deposits obtained from Cu without the addition of additive, which shows a dull red layer of copper. This demonstrated that the crystal size in this coating were typically smaller, and thus the coating smother, than for the Cu deposit produced without the NA additive, and which appeared as porous and dark deposits. Here, the thickness of the Cu coatings with/without additive were measured through cross-sectional morphologies via SEM, as shown in **Fig. 7c, f, i and l**, i.e., the right-hand images. It was found

that the average thickness of the pure additive-free Cu deposit was 10.06 μm , whereas with at 0.01, 0.03, and 0.05 M NA were about 8.86, 8.89, 3.04 μm , respectively, indicating a significant decline in the thickness and thus roughness (see **Fig. 8**) of the Cu deposit obtained with NA additive in a similar manner to Gu and co-workers [56]. This further supports the possibility of the additive being strongly adsorbed onto the mild steel substrate during Cu electroplating, inhibiting Cu nucleus formation as the active sites on the electrode surface become blocked, as implied by the CV profile and the EQCM data. In summary, it is clear that the data show that the concentration of NA additive has a significant effect on the growth process and on the Cu deposit morphology. The results noted here are in good agreement with previous work [57, 58].



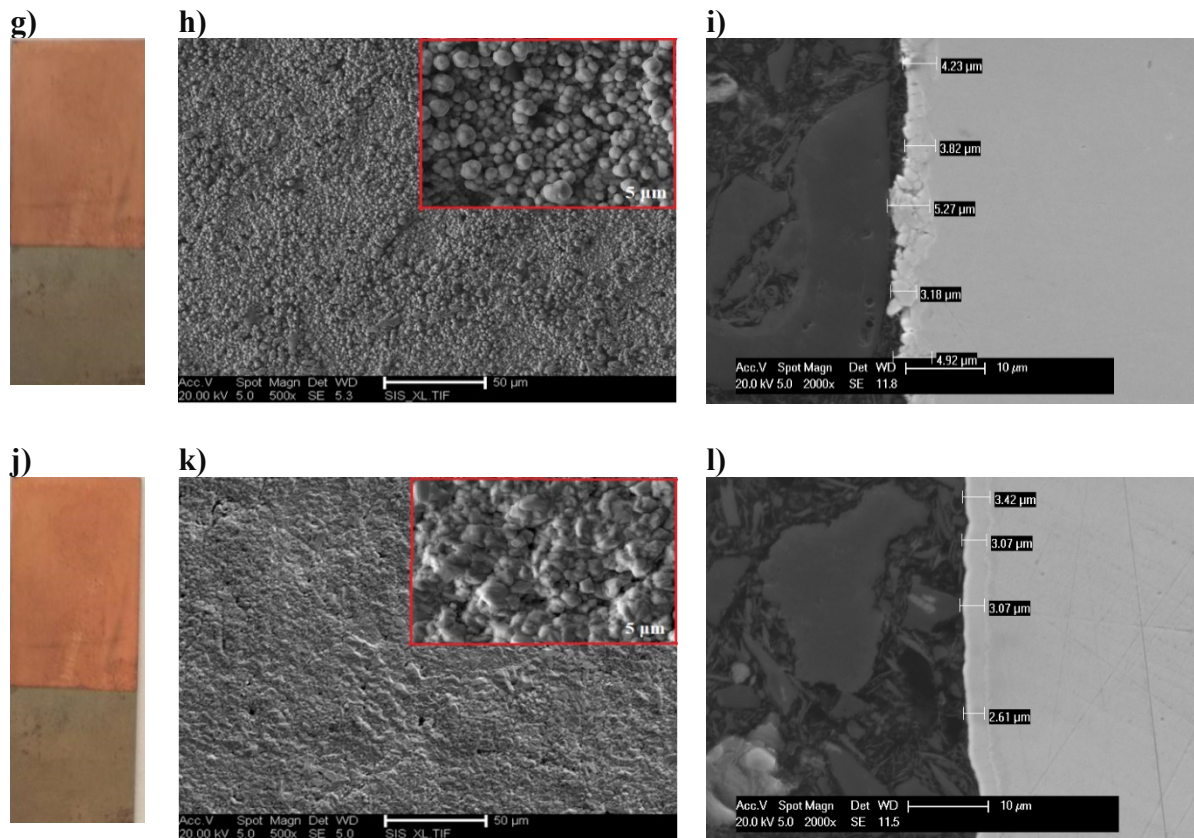


Fig. 7. Visual photos (left), SEM morphologies (middle) and cross-sections (right) of 0.3 M CuCl_2 deposits achieved from Ethaline 200 with and without various concentrations of NA at a current density of 2 mA cm^{-2} for 1 h on a mild steel substrate at 70°C . Images **a)**, **b)** and **c)** are for the Cu deposition without NA; **d)**, **e)** and **f)** are for the Cu deposition with the 0.01 NA additive; **g)**, **h)** and **i)** are for the Cu deposition with the 0.03 NA additive; and **j)**, **k)** and **l)** are for the Cu deposition with the 0.05 NA additive.

In this investigation, the topography and roughness of the Cu coatings obtained from Ethaline 200 at 70°C , both without and with the NA additive in various concentrations, were also characterised via the AFM technique, as illustrated in **Fig. 8**. The roughness of the Cu deposition without the NA additive was approximately 456 nm, decreasing significantly to approximately 177, 163, and 169 nm on use of 0.01, 0.03 and 0.05 M NA additive, respectively, with a corresponding decrease in surface roughness. From the AFM images we can see that the size of islands is smaller and thus roughness decreases with increasing concentration of additive in the plating bath compared to that observed from additive-free Cu deposits. Accordingly, the data suggest that NA additive affects

the deposition of Cu, and the action of this additive varies from the deposits prepared from additive-free electrolyte.

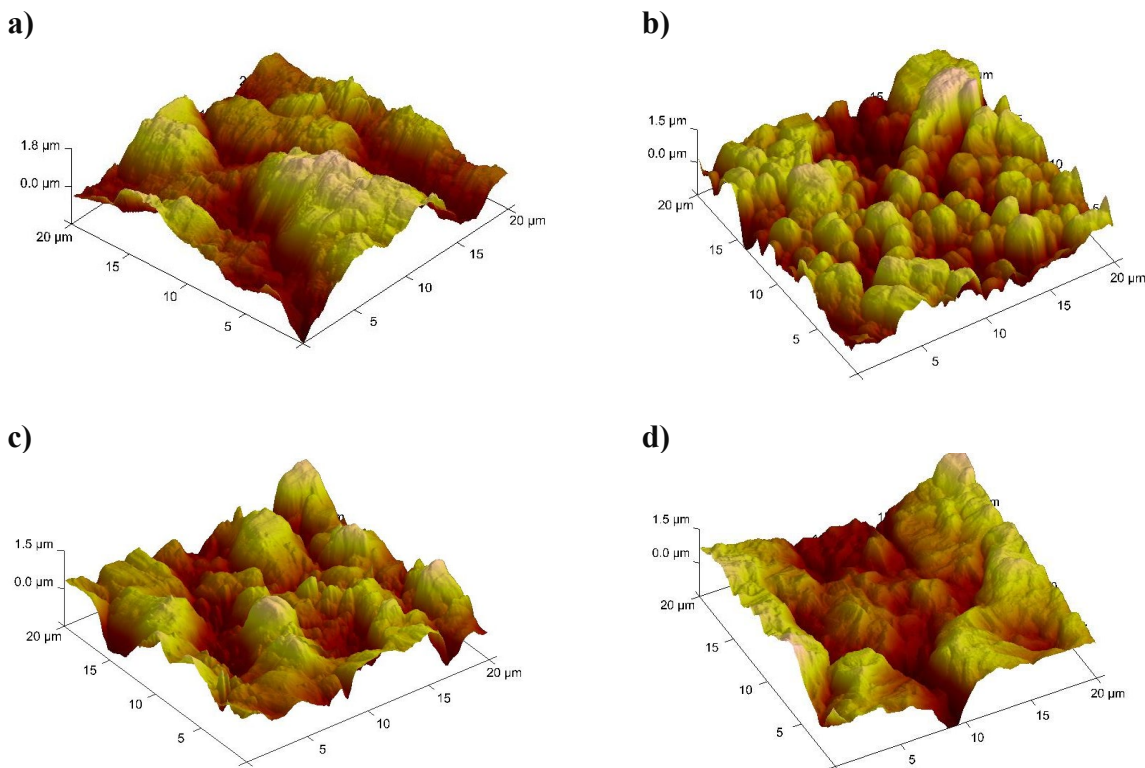


Fig. 8 AFM images of the surface morphology of the copper coating deposited by electrodepositing from Ethaline 200 with and without different concentrations of NA at a current density of 2 mA cm^{-2} on a mild steel at 70°C for 1 h. Images **a)** is for the Cu deposition without NA, while **b)**, **c)** and **d)** are for the Cu deposition with 0.01 M, 0.03 M, 0.05 M of NA additive, respectively.

3.6. X-Ray diffraction study

Fig. 9 illustrates the X-ray diffraction spectra for the Cu patterns found for 0.3 M $\text{CuCl}_2 \cdot 2\text{H}_2\text{O}$ in 1ChCl:2EG-based ionic liquid containing various concentrations of NA at 70°C on a mild steel substrate, applying a current density of 2 mA cm^{-2} for 1 h. As shown in **Fig. 9**, there are three main crystallographic orientations in all samples that appear at $2\theta = 43.36^\circ$, 50.44° , and 74.11° , indicative of the [111], [200] and [220] planes of copper, respectively, and as similar to those reported in previous studies [2, 59]. Moreover, all patterns show sharp peaks belonging to the crystalline phases of pure Cu. No shifts in the diffraction peaks were detected for the Cu deposits

when using the various concentrations of additive in comparison with Cu deposit without additive. However, a remarkable variation was detected for Cu electrodeposition from the system containing different concentrations of additive. It is obvious that the study shows that the amount of additive affects the XRD peak intensity, which decreases with the relative ratio of the additive to cupric ion. For example, the intensity of the [111] plane was reduced to 86%, 75%, and 41% when the deposition was performed with 0.01 M, 0.03 M and 0.05 M of NA additive in the plating bath, respectively, in comparison with deposits obtained from additive-free Cu, as shown in the insert in **Fig. 9**. A similar observation in terms of decrease in intensity was made for the [200] and [220] peaks when NA was added. It can be concluded that the addition of NA to the plating bath during Cu deposition alters in the crystallographic orientations of the Cu, which leads to a change in the deposition rates of the various crystal faces. This result suggests the addition of NA to the plating solution blocks crystal formation in the direction of the [111], [200] and [220] planes. This variation in the intensity of planes could be due to the adsorption of NA on these peaks during the crystal formation process.

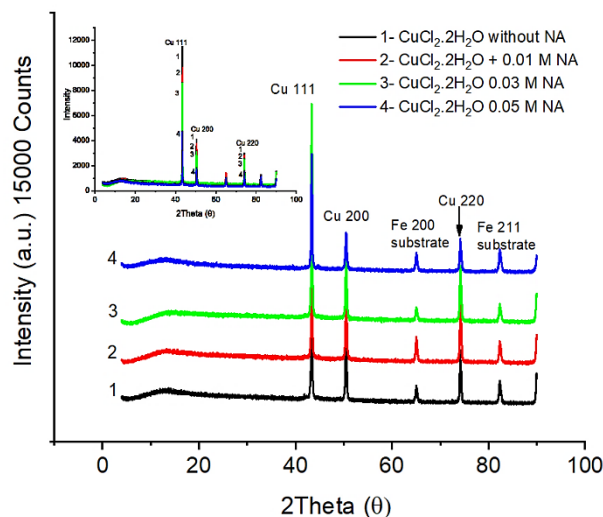


Fig. 9. XRD samples for 0.3 M $\text{CuCl}_2 \cdot 2\text{H}_2\text{O}$ coatings from Ethaline 200 containing different concentrations of NA additive between 0.01 and 0.5 M. The deposition processes were obtained over 1 h at a current of 2 mA cm^{-2} and at 70°C on mild steel plat

4. Conclusion

In this research, the successful electrodeposition of Cu with different concentrations of nicotinic acid as an additive from Ethaline 200 DES at 70°C on a mild steel substrate was investigated in

detail. The formation of Cu without/with NA was examined via various analytical techniques including UV-visible spectroscopy, cyclic voltammetry, chronocoulometry, and EQCM. Surface morphology, roughness and thickness were characterised via SEM and AFM while the crystal orientation was examined via XRD. The above techniques showed that there were clear changes between the responses for different concentrations of additive compared to the system without additive as a result of the complexity of the phases formed. As would be expected, the concentration of the additive in the plating bath is particularly significant, affecting the diffusion coefficient of the Cu deposition and the properties of the film. From the CVs, the diffusion coefficient for the Cu electrodeposition from a plating bath containing additive is reported above (see **Table 1**), and which was found to be less than that for pure Cu ($D = 4.86 \times 10^{-7} \text{ cm}^2 \text{ s}^{-1}$).

In addition, it was demonstrated that the NA additive was adsorbed onto active sites on the electrode surface, strongly limiting Cu deposition rates at cathodic potentials. Thus, using the mass-charge *in situ* method via EQCM, we also observed that the Cu growth current efficiencies decreased in a manner that was strongly dependent on the concentration of additive in the Cu-Ethaline solution, supporting the hypothesis of the active surface being inhibited during Cu deposition due to the additive adsorption onto the electrode substrate. It was also shown that smoothest surface morphologies and reduced roughness can be obtained from a system containing the nicotinic acid additive, in contrast to the system without this additive, as well as a brighter, adherent Cu coating being formed. It can be concluded that the act of using this additive was highly beneficial for the Cu coating in a choline chloride-ethylene glycol-based ionic liquid at 70°C, which is currently a significant contribution to new green techniques compared to the classical acidic or alkaline plating solutions.

Declaration of Competing Interest

The authors declare that they have no known competing financial interests or personal relationships that could have influenced the work reported in this paper.

Acknowledgment

This work has been sponsored by the MHESR, Iraq. The authors would like to acknowledge prof. Andy Abbott (University of Leicester) for helping and support.

References

- [1] M. Pasquale, L.M. Gassa, A.J. Arvia, Copper electrodeposition from an acidic plating bath containing accelerating and inhibiting organic additives, *Electrochim. Acta.* 53(20) (2008) 5891-5904.
- [2] M. Ibrahim, R. Bakdash, New non-cyanide acidic copper electroplating bath based on glutamate complexing agent, *Surf. Coat. Technol.* 282 (2015) 139-148.
- [3] S. Miura, H. Honma, Advanced copper electroplating for application of electronics, *Surf. Coat. Technol.* 169 (2003) 91-95.
- [4] R. Bernasconi, M. Zebarjadi, L. Magagnin, Copper electrodeposition from a chloride free deep eutectic solvent, *J. Electroanal. Chem.* 758 (2015) 163-169.
- [5] P. Sebastian, E. Valles, E. Gómez, Copper electrodeposition in a deep eutectic solvent. First stages analysis considering Cu (I) stabilization in chloride media, *Electrochim. Acta* 123 (2014) 285-295.
- [6] D. Grujicic, B. Pesic, Electrodeposition of copper: the nucleation mechanisms, *Electrochim. Acta.* 47(18) (2002) 2901-2912.
- [7] J. Zhang, A. Liu, X. Ren, J. Zhang, P. Yang, M. An, Electrodeposit copper from alkaline cyanide-free baths containing 5, 5'-dimethylhydantoin and citrate as complexing agents, *Rsc Adv.* 4(72) (2014) 38012-38026.
- [8] W. Canning, Co, *Handbook on Electroplating: Polishing, Bronzing and Lacquering*, W. Canning & Company 1966.
- [9] D. Stoychev, C. Tsvetanov, Behaviour of poly (ethylene glycol) during electrodeposition of bright copper coatings in sulfuric acid electrolytes, *J. Appl. Electrochem.* 26(7) (1996) 741-749.
- [10] L. Oniciu, L. Mureşan, Some fundamental aspects of levelling and brightening in metal electrodeposition, *J. Appl. Electrochem.* 21(7) (1991) 565-574.
- [11] Y.-M. Lin, S.C. Yen, Effects of additives and chelating agents on electroless copper plating, *Appl. Surf. Sci.* 178(1-4) (2001) 116-126.
- [12] L. Mirkova, C. Nanev, The levelling mechanism during bright acid copper plating, *Surf. Technol.* 15(3) (1982) 181-190.
- [13] E.L. Smith, A.P. Abbott, K.S. Ryder, Deep eutectic solvents (DESs) and their applications, *Chem. Rev.* 114(21) (2014) 11060-11082.

- [14] A.P. Abbott, G. Capper, D.L. Davies, R.K. Rasheed, V. Tambyrajah, Novel solvent properties of choline chloride/urea mixtures, *Chem. Commun.* (1) (2003) 70-71.
- [15] H.F. Alesary, H.K. Ismail, N.M. Shiltagh, R.A. Alattar, L.M. Ahmed, M.J. Watkins, K.S. Ryder, Effects of additives on the electrodeposition of ZnSn alloys from choline chloride/ethylene glycol-based deep eutectic solvent, *J. Electroanal. Chem.* 874 (2020) 114517.
- [16] X. Ren, X. Zhu, C. Xu, Y. Hua, Q. Zhang, H. Liu, X. Wang, M. Huang, S. Wang, J. Ru, The electrodeposition of amorphous/nanocrystalline Ni–Cr alloys from ChCl–EG deep eutectic solvent, *J. Electrochem. Soc.* 167(6) (2020) 062502.
- [17] C. Lei, H.F. Alesary, F. Khan, A.P. Abbott, K.S. Ryder, Gamma-phase Zn-Ni alloy deposition by pulse-electroplating from a modified deep eutectic solution, *Sur. Coat. Technol.* 403 (2020) 126434.
- [18] N.M. Pereira, C.M. Pereira, J.P. Araujo, A.F. Silva, Zinc electrodeposition from deep eutectic solvent containing organic additives, *J. Electroanal. Chem.* 801 (2017) 545-551.
- [19] A.P. Abbott, A. Ballantyne, R.C. Harris, J.A. Juma, K.S. Ryder, G. Forrest, A comparative study of nickel electrodeposition using deep eutectic solvents and aqueous solutions, *Electrochim. Acta.* 176 (2015) 718-726.
- [20] A.Y. Al-Murshedi, A. Al-Yasari, H.F. Alesary, H.K. Ismail, Electrochemical fabrication of cobalt films in a choline chloride–ethylene glycol deep eutectic solvent containing water, *Chem. Pap.* 74(2) (2020) 699-709.
- [21] A.P. Abbott, G. Capper, K.J. McKenzie, A. Glidle, K.S. Ryder, Electropolishing of stainless steels in a choline chloride based ionic liquid: an electrochemical study with surface characterisation using SEM and atomic force microscopy, *Phys. Chem. Chem. Phys.* 8(36) (2006) 4214-4221.
- [22] A.P. Abbott, G. Capper, K.J. McKenzie, K.S. Ryder, Voltammetric and impedance studies of the electropolishing of type 316 stainless steel in a choline chloride based ionic liquid, *Electrochim. Acta.* 51(21) (2006) 4420-4425.
- [23] I.B. Qader, J.H. Kareem, H.K. Ismail, H.K. Mahmood, Novel phenolic deep eutectic solvents for desulfurisation of petrodiesel, *Karbala International Journal of Modern Science* 7(1) (2021) 12.

- [24] H.K. Ismail, H.F. Alesary, A.Y. Al-Murshedi, J.H. Kareem, Ion and solvent transfer of polyaniline films electrodeposited from deep eutectic solvents via EQCM, *J. Solid State Electrochem.* 23(11) (2019) 3107-3121.
- [25] H.K. Ismail, H.F. Alesary, M.Q. Mohammed, Synthesis and characterisation of polyaniline and/or MoO₂/graphite composites from deep eutectic solvents via chemical polymerisation, *J. Polym. Res.* 26(3) (2019) 65.
- [26] A.P. Abbott, K. El Ttaib, G. Frisch, K.J. McKenzie, K.S. Ryder, Electrodeposition of copper composites from deep eutectic solvents based on choline chloride, *Phys. Chem. Chem. Phys.* 11(21) (2009) 4269-4277.
- [27] P. Valverde, T. Green, S. Roy, Effect of water on the electrodeposition of copper from a deep eutectic solvent, *J. Appl. Electrochem.* 50 (2020) 699–712.
- [28] P. De Vreese, N.R. Brooks, K. Van Hecke, L. Van Meervelt, E. Matthijs, K. Binnemans, R. Van Deun, Speciation of copper (II) complexes in an ionic liquid based on choline chloride and in choline chloride/water mixtures, *Inorg. Chem.* 51(9) (2012) 4972-4981.
- [29] J.M. Hartley, C.M. Ip, G.C. Forrest, K. Singh, S.J. Gurman, K.S. Ryder, A.P. Abbott, G. Frisch, EXAFS study into the speciation of metal salts dissolved in ionic liquids and deep eutectic solvents, *Inorg. Chem.* 53(12) (2014) 6280-6288.
- [30] K. Kondo, N. Yamakawa, Z. Tanaka, K. Hayashi, Copper damascene electrodeposition and additives, *J. Electroanal. Chem.* 559 (2003) 137-142.
- [31] H.K. Ismail, Electrodeposition of a mirror zinc coating from a choline chloride-ethylene glycol-based deep eutectic solvent modified with methyl nicotinate, *J. Electroanal. Chem.* 876 (2020) 114737.
- [32] K. Kondo, T. Matsumoto, K. Watanabe, Role of additives for copper damascene electrodeposition: Experimental study on inhibition and acceleration effects, *J. Electrochem. Soc.* 151(4) (2004) C250.
- [33] L. Muresan, S. Varvara, G. Maurin, S. Dorneanu, The effect of some organic additives upon copper electrowinning from sulphate electrolytes, *Hydrometallurgy* 54(2-3) (2000) 161-169.
- [34] J.A. Juma, H.K. Ismail, W.O. Karim, S.J. Salih, High quality mirror finish fabrication of nickel electrodeposited using hydantoin from a mixture of choline chloride-ethylene glycol, *Arab. J. Chem.* 14(3) (2021) 102966.

- [35] N.A. Shaheen, I. Mahesh, M.B. Vukmirovic, R. Akolkar, Hysteresis effects and roughness suppression efficacy of polyethylenimine additive in Cu electrodeposition in ethaline, *Electrochem. Commun.* 115 (2020) 106721.
- [36] A.M. Popescu, A. Cojocaru, C. Donath, V. Constantin, Electrochemical study and electrodeposition of copper (I) in ionic liquid-reline, *Chem. Res. Chin. Univ.* 29(5) (2013) 991-997.
- [37] N. Panyoyai, A. Bannikova, D.M. Small, R.A. Shanks, S. Kasapis, Diffusion of nicotinic acid in spray-dried capsules of whey protein isolate, *Food Hydrocoll.* 52 (2016) 811-819.
- [38] X. Shen, N. Sinclair, J. Wainright, R. Akolkar, R. Savinell, Evaluating and developing a reliable reference electrode for choline chloride based deep eutectic solvents, *J. Electrochem. Soc.* 167(8) (2020) 086509.
- [39] A.P. Abbott, G. Frisch, J. Hartley, K.S. Ryder, Processing of metals and metal oxides using ionic liquids, *Green Chem.* 13(3) (2011) 471-481.
- [40] J. Urbańska, H. Podsiadły, Interaction of niacin with copper ions, *Polyhedron* 60 (2013) 130-139.
- [41] K. Waizump, M. Takuno, N. Fukushima, H. Masuda, Structures of pyridine carboxylate complexes of cobalt (II) and copper (II), *J. Coord. Chem.* 44(3-4) (1998) 269-279.
- [42] A.-M. Popescu, V. Constantin, A. Cojocaru, M. Olteanu, Electrochemical behaviour of copper (II) chloride in choline chloride-urea deep eutectic solvent, *Rev. Chim.(Bucharest)* 62(2) (2011) 206-211.
- [43] A. Abbott, G. Frisch, S. Gurman, A. Hillman, J. Hartley, F. Holyoak, K. Ryder, Ionometallurgy: designer redox properties for metal processing, *Chem. Commun.* 47(36) (2011) 10031-10033.
- [44] J.R. Brusas, E.M.B.D. Pena, Hygroscopicity of 1: 2 Choline chloride: Ethylene glycol deep eutectic solvent: A hindrance to its electroplating industry adoption, *J. Electrochem. Sci. Technol.* (2021). <https://doi.org/10.33961/jecst.2020.01522>
- [45] J.O.M. Bockris, A.K.N. Reddy, *Modern Electrochemistry: Ionics*, 2 ed., Springer US, New York, 1998.
- [46] A.P. Abbott, A. Ballantyne, R.C. Harris, J.A. Juma, K.S. Ryder, Bright metal coatings from sustainable electrolytes: the effect of molecular additives on electrodeposition of nickel from a deep eutectic solvent, *Phys. Chem. Chem. Phys.* 19(4) (2017) 3219-3231.

- [47] M. Schlesinger, M. Paunovic, *Modern Electroplating*, Wiley 2011.
- [48] H.L.Z.R.G. Min, Y.F.Z.X.S. Kai, Z.S. Min, Effects of nicotinic acid on copper electrodeposition in acid sulphate [J], *Acta Physico-chimica Sinica* 7 (2002).
- [49] L. Korson, W. Drost-Hansen, F.J. Millero, Viscosity of water at various temperatures, *J. Phys. Chem.* 73(1) (1969) 34-39.
- [50] P.M.S. Monk, *Fundamentals of Electroanalytical Chemistry*, Wiley 2008.
- [51] A. Liu, Z. Shi, R.G. Reddy, Mechanism study of Cu-Zn alloys electrodeposition in deep eutectic solvents, *Ionics* 26 (2020) 3161–3172.
- [52] D.R. Crow, *Principles and Applications of Electrochemistry*, CRC Press 2017.
- [53] G. Sauerbrey, Verwendung von Schwingquarzen zur Wägung dünner Schichten und zur Mikrowägung, *Zeitschrift für physik* 155(2) (1959) 206-222.
- [54] H.F. Alesary, S. Cihangir, A.D. Ballantyne, R.C. Harris, D.P. Weston, A.P. Abbott, K.S. Ryder, Influence of additives on the electrodeposition of zinc from a deep eutectic solvent, *Electrochim. Acta.* 304 (2019) 118-130.
- [55] K. Haerens, E. Mattheijs, K. Binnemans, B. Van der Bruggen, Electrochemical decomposition of choline chloride based ionic liquid analogues, *Green Chem.* 11(9) (2009) 1357-1365.
- [56] C. Gu, Y. You, X. Wang, J. Tu, Electrodeposition, structural, and corrosion properties of Cu films from a stable deep eutectics system with additive of ethylene diamine, *Sur. Coat. Technol.* 209 (2012) 117-123.
- [57] Z. Liu, S. Zein El Abedin, N. Borisenko, F. Endres, Influence of an additive on zinc electrodeposition in the ionic liquid 1-ethyl-3-methylimidazolium trifluoromethylsulfonate, *ChemElectroChem* 2(8) (2015) 1159-1163.
- [58] H.F.N. Al-Esary, *Influence of additives on electrodeposition of metals from deep eutectic solvents*, University of Leicester, 2017.
- [59] H. Nady, M. Negem, Ni–Cu nano-crystalline alloys for efficient electrochemical hydrogen production in acid water, *RSC Adv.* 6(56) (2016) 51111-51119.